Reanalysis of monkey head concussion experiment data using a novel monkey finite element model to develop brain tissue injury reference values

Jacobo Antona-Makoshi[1], Johan Davidsson[2], Susumu Ejima[3], Koshiro Ono[4]

Abstract A new method has been applied to develop a Finite Element (FE) model of the head- neck complex of Macaque monkey from medical images. The skull, brain and flesh have been validated based on tissue and component experimental data from literature. The kinematics of the head during occipital impacts have been validated against a sub-set of head impact experiments carried out in the past at the Japan Automobile Research Institute (JARI). The validated model has been used to simulate 19 occipital impacts case-by-case. The correlation between obtained peak values for a number of mechanical parameters of the different brain regions and the occurrence of concussion in the experiments was analysed. Maximum principal strain in the brainstem showed significant correlation to concussion; 21% strain was associated with a probability of 50% risk for concussion. The developed model and the presented results constitute the first step towards the development of a tissue level injury criterion for humans that is based on experimental animal data.

Keywords Concussion, finite element model, head, monkey experiments, traumatic brain injury.

I. INTRODUCTION

Traumatic Brain Injuries (TBIs) are one of the major public health problems in all parts of the world. The consequences following these injuries are serious and frequently present throughout life. Many of these injuries are caused by a combination of rotational and linear accelerations of the head in leisure and sports related accidents, or due to traffic accidents. It is estimated that the latter comprises more than half of the 1.3 million annual TBI victims [1].

Despite the efforts spent by the research community in the last decades, two main factors contribute to the progress advancing slower than expected at [2]:

- The complexity of brain injuries including difficulties to provide detailed diagnosis, localisation and quantification of injury extent, and determine the loads that produced the injuries.
- The necessity to study brain injuries in living subjects to account for the biological reactions to loads.

To overcome these difficulties, experiments on Non-Human Primates (NHP) to investigate human brain injury tolerance were common in the past [3]-[6]. One experimental series was performed at the JARI in the late 1970's. All tests were conducted under the animal care regulations in effect at that time and with the approval of major academic societies. The original experimental series consisted of four main groups with different impact set-ups and injury levels. The first three groups (A, B and C) consisted of sagittal impacts of different nature and severity [6]. A fourth group of coronal impacts was performed and presented separately [7][8]. The most important outcome of these experiments was the JARI Human Head Tolerance Curve (JHTC) which present levels for human tolerance of concussion. It was also found that concussion type injury was associated with impacts below the thresholds for skull fracture.

Despite the value of these and other monkey trauma experiments, two important aspects associated with the method still require additional attention.

Firstly, the monkey trauma experiments failed to show the causation of the brain injuries. An improved understanding of the causation is required, e.g., how the head-neck complex was accelerated, how the skull was deformed, and how the brain deformed and interacted with the skull. These crucial aspects need to and can be clarified and quantified using FE models of the test subjects.

Jacobo Antona-Makoshi is a researcher at the Japan Automobile Research Institute (JARI) and PhD Student at Chalmers University of Technology, Sweden (Ph: +81-29-856-0885, fax: +81-29-856-1121, ajacobo@jari.or.jp). Johan Davidsson is Assistant Professor in Impact Biomechanics at Chalmers University, Sweden. Susumu Ejima is a research manager at JARI, Japan. Koshiro Ono is the Executive Research Adviser & Research Director at JARI, Japan.

Secondly, despite the analogy in mechanical, physiological and biological responses of monkeys and humans, the experimental results have to be scaled to apply to humans. The scaling approaches used in the past [9][10] were based on assumptions that have been criticised and scarcely validated [11].

To address these two aspects, an FE model of the head and neck of a monkey was created, validated and applied to simulate a sub-set of the head occipital trauma experiments performed in the past at JARI [6]. This work is an effort to develop a more robust method for scaling brain injury data from NHP to humans and to develop an improved brain injury threshold that has the potential to reduce the number of brain injuries due to closed head impacts. The aim of this specific work is two-fold:

- To better understand the loading mechanisms of the brain that lead to brain injury.
- To identify the key strain-based parameters at each region of the brain that correlate with the brain symptoms following an injury produced in the experiments.

II. METHODOLOGY

The methodology of the work presented here consists of five steps:

1. Reanalysis of a consistent sub-set of the historical JARI head trauma experimental data [6];
2. Development of a monkey head-neck FE model based on new medical images;
3. Validation of the monkey FE model based on literature data as well as the historical JARI data;
4. Simulation of 19 selected occipital head impacts; and
5. Analysis of the statistical correlation between the strain-based parameters obtained in the simulations for different brain regions and the occurrence of concussion in the experiments.

Reanalysis of historical JARI head trauma experimental data

Figure 1 shows an illustration of the experimental equipment used in the historical JARI head trauma experiments and a sketch of the occipital impact set-up which is the focus of this work [12]. This group consisted of a series of non-fatal direct impacts that resulted in combined rotational and translational head accelerations. The data available for the selected cases include linear and rotational head accelerations, high speed videos, photographs from pathological examinations and records of symptoms and injuries. Pathological injuries scored were SubArachnoid Hemorrhage (SAH) and SubDural Hematoma (SDH). The severity of a concussion was evaluated by measuring changes in vital functions such as loss of corneal reflex, cease of respiration and blood pressure changes. The definition of concussion used was in accordance with the definitions provided at the time of the experiments by the Committee on Terminology in Neurotraumatology of the World Federation of Neurosurgical Societies [13].

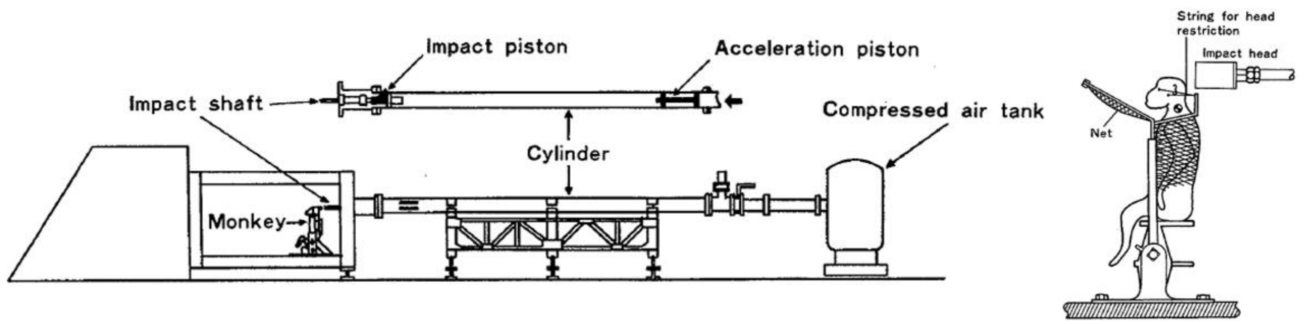

Fig. 1. Illustration of trauma producing equipment (Left) and illustration of how the direct occipital impact was produced (Right). Image reprinted from [12] by permission.

To generate a consistent data sub-set suitable for the simulation work, the following selection criteria were applied to the experimental data:

- Only direct occipital impact in the sagittal plane was included;
- The specimens were either Macaca Fuscata (Japanese monkey) or Macaca Mulatta (Rhesus monkey);
- The experiment resulted in no skull fracture; and
- The head resultant linear acceleration curves were available.

A preliminary group of 21 cases fulfilled the selection criteria. After a revision of the high speed videos and the reports, 2 cases were discarded because experimental artefacts may have affected the measured head accelerations. Table I presents the final 19 selected cases. The experimental numbering was kept as in the original publications so more detailed information on the experimental equipment, method and the quantified injury output can be recognised in the original publication [6]. The impacts produced peak resultant head accelerations ranging from 2,100 to 13,400 m/s^2 and impact durations from 4.0 to 10.1 ms. The impact duration was expressed as a 10% level interval against the maximum of the resultant acceleration as described in [7]. The average body mass of the macaques used for the final 19 selected cases was 6.2 kg.

TABLE I
SUB-GROUP OF 19 CASES REANALYSED FROM [6]

Exp. No	Subject	Impact Velocity (m/s)	Impactor Rubber type (**)	Impact Stroke (mm)	Head Acceleration Peak (m/s2)	Head Acceleration Avg (m/s2)	Head Acceleration Duration (ms)	Rotational Acceleration Peak (krad/s2)	Rotational Acceleration Avg (krad/s2)	Rotational Acceleration Duration (ms)	Concussion Occurrence (Grade)
311	2	10.9	B	20	3,000	1,800	4.6	51	17	5.1	No (0)
312	2	14.4	B	20	5,800	3,500	3.3	64	23	4.0	No (0)
313	2	16.3	B	20	5,000	3,200	4.3	51	20	4.9	Yes (I)
314	2	18.0	B	20	6,500	3,700	4.9	115	-	-	Yes (I)
316	2	19.8	B	20	6,900	4,000	3.1	83	28	4.2	No (0)
321	9	21.7	A	30	8,800	3,700	4.9	105	43	7.4	Yes (II)
322	10	15.5	D	30	6,900	2,900	3.9	171	51	9.9	Yes (I)
344	18	10.8 (*)	E	40	4,600	2,300	6.9	-	-	-	No (0)
345	18	17.0	E	40	7,100	2,700	6.6	89	32	7.6	Yes (I)
356	12	6.8	E	60	2,200	1,400	12.2	20	8	8.9	No (0)
357	12	7.5	E	90	2,100	1,400	12.3	13	6	9.1	Yes (I)
358	12	11.5	E	90	3,800	2,200	13.1	38	12	8.1	No (0)
359	12	13.7	E	60	4,700	2,350	14	47	16	10.1	Yes (II)
360	12	16.4	E	60	5,800	2,550	12.6	95	22	6.1	Yes (II)
362	777	10.8	E	10	8,300	5,100	2.2	55	20	6.3	No (0)
363	777	13.4	E	10	13,400	6,800	2.4	179	76	4.5	Yes (I)
370	44	8.0	E	30	2,900	1,400	13.5	46	12	8.7	No (0)
371	44	7.3	E	20	2,200	1,400	5.8	14	8	6.8	No (0)
372	44	8.5	E	25	3,000	1,800	6.9	41	10	8.2	No (0)

(*) Impact velocity of case 344 was not reported in the original publication. An estimate based on the high speed video showed an impactor speed of approximately 10.8 m/s, which coincides with the average impactor speed for the cases in which no concussion was observed.
(**) The rubber blocks mounted to the impactor had five different material properties. 'A' corresponds with the stiffest and 'E' with the softest. The load-deflection curves of the different rubber materials were provided in [6].

To quantify the concussion grade produced by the impact, the following three criteria were used during the time of the experiments:

1. Persistent loss of corneal reflex for at least 20 seconds after the impact;
2. Cease of respiration for at least 20 seconds after the impact; and
3. Two levels of blood pressure disturbance following the impact.

In the original study, concussion grade 0 was assigned when none of the three criteria applied. Concussion grades I, II or III were assigned when one, two or three of the criteria applied, respectively. In the work presented in this article, all the cases that presented concussion were grouped together as shown in Table I. The resultant acceleration experimental curves for each case were digitised from the original reports and grouped according to injury occurrence (Figures 2 and 3). The resulting average impact velocities for these two groups were 10.8 m/s and 15.5 m/s, respectively.

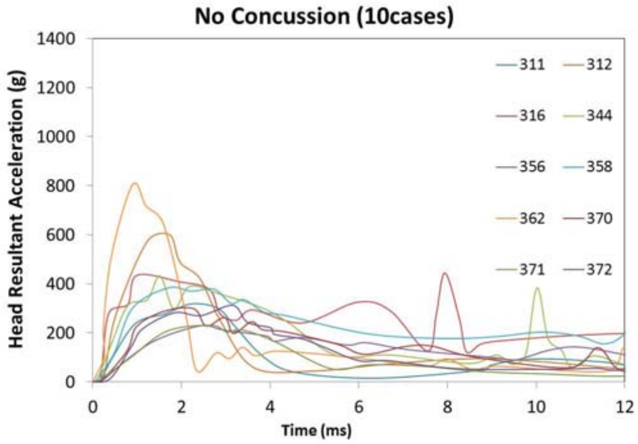

Fig 2. Head resultant acceleration curves for the experimental cases without concussion.

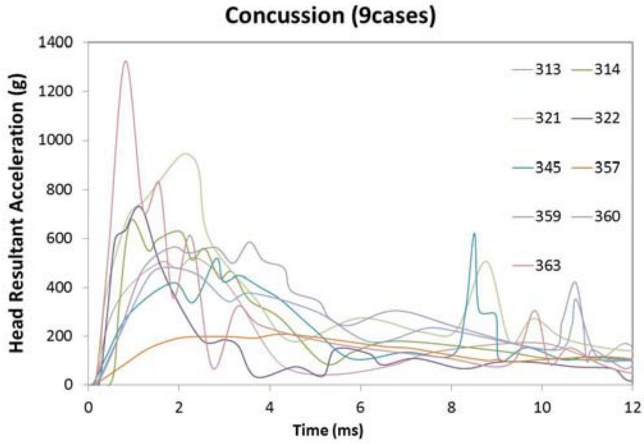

Fig 3. Head resultant acceleration curves for the experimental cases with concussion.

Development of monkey head-neck FE model

An FE model of the head and neck of a macaque was developed by combining a Rhesus monkey brain digital atlas in stereotactic coordinates [14], and an original set of Computed Tomography (CT) scans and Magnetic Resonance Images (MRI) from a subject of Macaca Fuscata. The images were taken from an anaesthetised specimen at the Primate Research Institute of Kyoto University (KUPRI) imaging facilities. The procedures to care and treat the animal and the purpose of the usage of the images were approved by the Animal Welfare and Animal Care Committee ethics panel of the KUPRI (Permission 2011-134, 7 June, 2011). A Toshiba Asteion 4 machine was used to capture the CT scans with 0.5 mm slice thickness and 0.2 mm slice distance. The CT data set (id: PRICT-379, specimen Mff2115) is available from the Digital Morphology Museum of KUPRI [15]. For the MRI, a 0.2 Tesla GE Signa Profile machine was used to capture 1 mm thick slices with 1 mm distance.

The specimen from which the images were captured was a 5 years old female with a body mass of 7.9 kg. A preliminary analysis of the dimensions of the skull measured from the images showed that the skull external dimensions and profile of thicknesses in the sagittal plane were very close to one of the two specimens from which compression experimental data were available in literature [16].

Several commercial software programmes were used for the digitisation of the brain atlas (GetData Graph Digitizer), segmentation of the medical images (Simpleware v4.2) and construction of a mesh (Hypermesh v11.0, SimLab and SimLab Kubrix). For the simulation work presented later, LS-Dyna (mpp971s R5.1.1) was used.

Figure 4 illustrates the development process of the monkey model described below.

The geometry of the skull was obtained from the CT images and segmented prior to meshing. An accelerated meshing process was utilised to obtain a hexahedral mesh of high geometrical accuracy of the skull. The volume representing the scalp and the soft tissue surrounding the cervical vertebrae was taken from the same images and meshed with a rapid tetrahedral mesh generation method.

To develop the mesh of the brain, a different technique was used aiming at a mesh of quality good enough to sustain severe loading conditions. The contours of the brain regions of interest in 58 coronal 1 mm equidistant sections of the brain, obtained from the Rhesus monkey brain Atlas [14], were identified and digitised in a similar way as described by [17] for the development of a rat brain FE model. The digitised contours were imported as point data into the meshing software. The points were used to define lines, planes and volumes that allowed building a hexahedral mesh. Since the dimensions of the Atlas' brain did not exactly correspond to the dimensions of the intracranial space of the skull from the CT scan, one more step was required to adjust the geometry of the brain mesh. To do this, the contours of the brain regions of interest and the cerebrospinal fluid space from the MR images were segmented and digitised. The FE mesh based on the Atlas and the segmented brain from the MR images were imported into the same software. Then, the FE mesh of each brain region was morphed to fit the volume of the corresponding brain region obtained from the processed MR images.

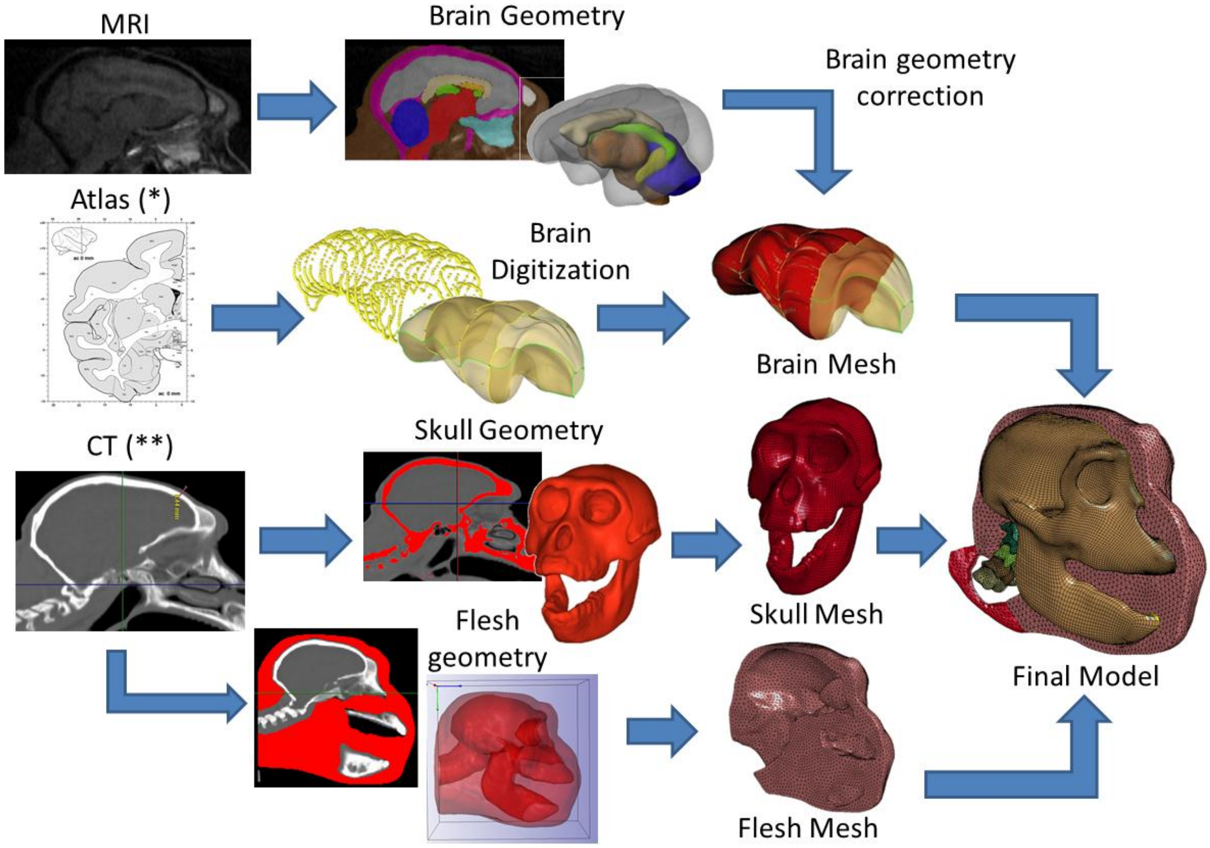

Fig. 4. JARI monkey head-neck FE model development process. (*) taken from the brain atlas available at [14]. (**) CT images available at [15]

The final model, shown in Figure 5, consists of 356,567 elements. It includes and differentiates between the skull and scalp, cerebrum, corpus callosum, brainstem, cerebellum, meninges, falx cerebri, tentorium, and the cerebrospinal fluid. The neck includes the cervical spine, the first five cervical vertebrae and the surrounding soft tissue. The skull mesh is made of 112,548 hexahedral elements with an average size of 0.9 mm. The brain is meshed with 21,750 hexahedral elements of approximately 1.8 mm. The flesh and the neck are built with 124,149 tetrahedral elements of 2 mm size.

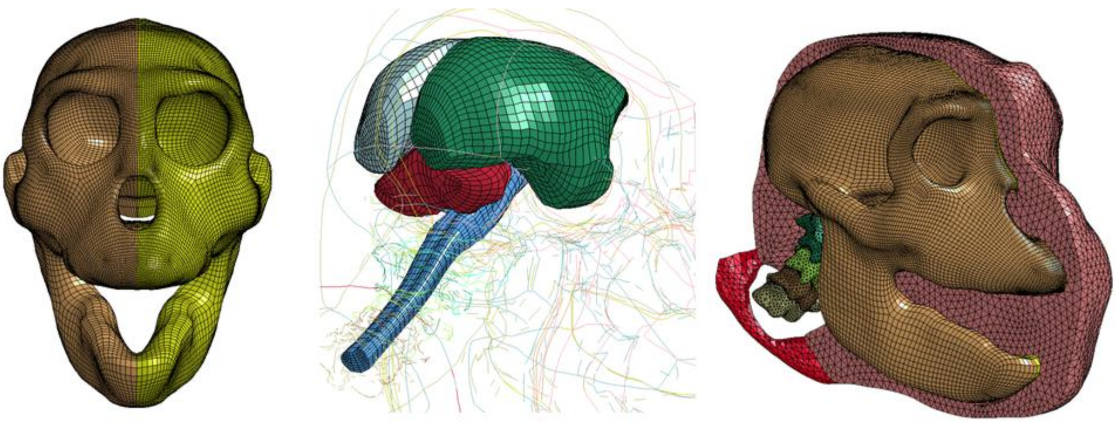

Fig 5. Pictures of the skull (left), the brain (middle) and the final mounted model (right). (In the picture of the final model, part of the flesh has been removed for visibility reasons)

Validation of monkey FE model; material modelling

The material properties of the brain regions and the scalp were validated against macaque tissue experiments from different sources [18]-[21]. For the skull bone, experimental data from compression tests of square cuts of skull bone tissue from Rhesus monkey by [18] was used. To define elastic properties of the dura mater, experimental data from human dura mater in tension [20] was used. Table II lists the material models, the material parameters and the references for each part of the FE model.

TABLE II
MONKEY FE MODEL MATERIAL PROPERTIES

	Material model	Material properties	Source
Scalp and neck underlying muscle tissue	Fu Chang foam	Experimental stress-strain curves at 3 strain rates	Monkey fresh scalp tissue in compression [18][19]
Skull bone	Piecewise linear plasticity	E = 6.48 GPa, US = 92.4 MPa	Monkey skull tissue compression in tangential direction [20]
Dura mater	Elastic	E = 40 MPa	Human dura matter in tension [20]
Cerebrum, corpus callosum, cerebellum	General viscoelastic	G0 = 10300 Pa, G1 = 3700 Pa, tau = 100 s^{-1}	Monkey brain tissue in compression [18][19]
Brainstem	General viscoelastic	G0 = 18540 Pa, G1 = 6660 Pa, tau = 100 s^{-1}	Material characterisation of swine brainstem tissue [21]

E = Young modulus, US = Ultimate Strength, K = Bulk modulus, G0 = Short term modulus, G1 = Long term modulus, tau = decay constant

Scalp tissue

To verify the mesh type and size, as well as the material properties of the scalp and the underlying muscle complex tissue of the FE model, Rhesus monkey fresh scalp tissue cylindrical compression tests by [18] were simulated. In the experiments, 10 mm height and 12.5 mm diameter cylindrical tissue specimens were subjected to compression at different speeds. To simulate the experiments, cylinders of tetrahedral elements of approximately the same size as the monkey FE model, were generated. While constraining the displacements of the nodes on the base of the cylinder, the displacement of the nodes on the upper surface were prescribed in compressive direction at different speeds. Figure 6 shows the stress-strain experimental curves digitised from the original publications and used as input material properties, in comparison with the results from the simulated experiments at strain rates of 1, 10 and 65 s^{-1}, respectively.

Brain tissue

To verify that the mesh type, size and material properties used for the brain tissue behave in accordance with the only source of monkey brain tissue experimental data found in literature [18][19], compressive relaxation experiments were simulated. In this case, cylindrical specimens of 6.35 mm height and 12.5 mm diameter were used. For this, a model of the cylindrical specimens made of hexahedral elements of approximately the same size as in the monkey brain model was created. In this case, while the nodes on the base were constrained, the nodes on the upper surface were subjected to a ramp-and-hold prescribed motion in compressive direction. Figure 7 shows the experimental stress-time relaxation modulus in comparison with the results from the simulated experiment. According to [21], the relaxation moduli for the brainstem were assumed to be 80% higher than the cerebrum.

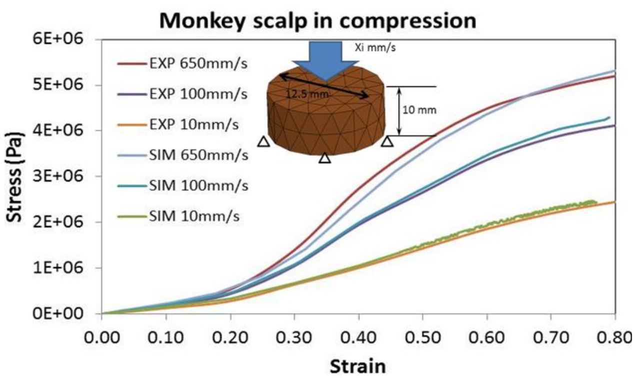

Fig. 6. Stress as a function of strain, simulation vs. experimental results of monkey fresh scalp tissue compression tests at three different strain rates.

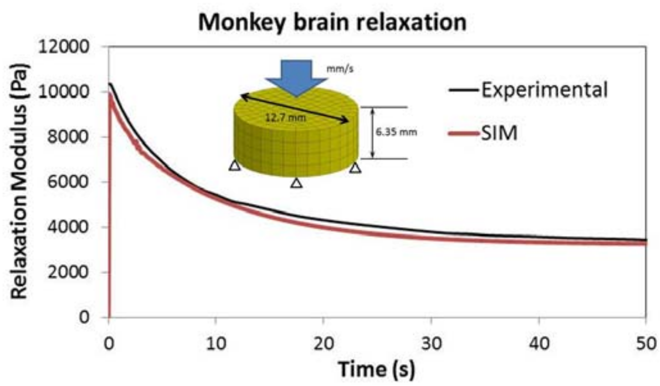

Fig. 7. Relaxation modulus as a function of time, simulation vs. experimental data of monkey brain tissue relaxation tests in compression.

Validation of monkey FE model; experimental data

Quasi-static skull bone compression

The skull bone material properties obtained from compression tests of small square cuts of skull bone [20] were implemented in the skull FE model and structural skull quasi-static compression tests in the sagittal direction from [16] were simulated. In the experiments, the skull was loaded by two cylinders (Figure 5) while strain was measured at 4 different locations. Three strain gage rosettes (Right, Left and Front) were located in the upper part of the skull, 25 mm from the bregma point. A fourth rosette (Occ) was placed on the occipital bone at 18 mm of the posterior part of the foramen magnum. Figure 8 shows the results for the force-strain curves at the experiments and the simulation results at the four different locations. Figure 9 shows a representation of the different strain values showing the pattern of areas of the skull subjected to higher strains during the anterior-posterior loading.

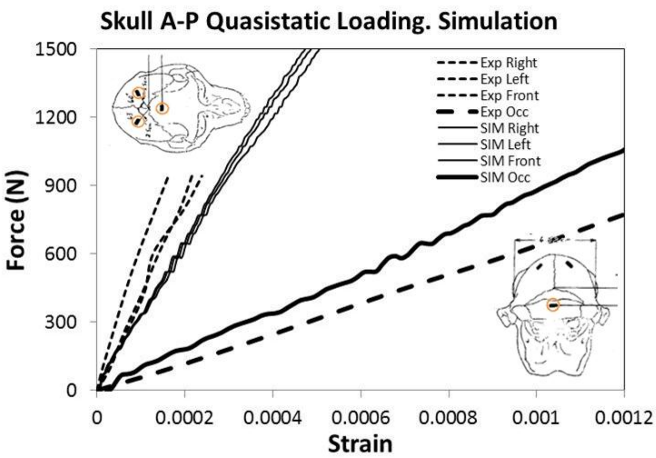

Fig. 8. Experiment vs. simulation force-strain curves at four locations of the skull

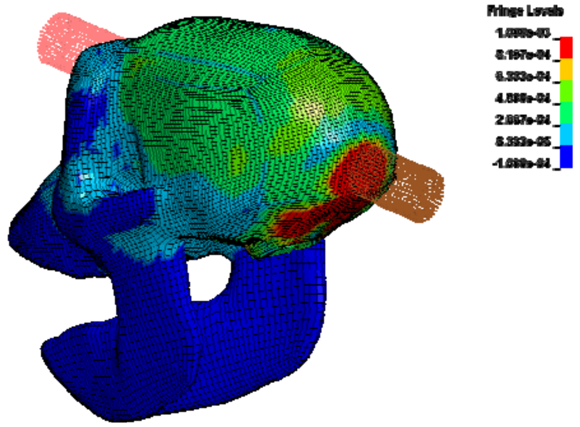

Fig. 9. Fringe plots for strain at the simulation of monkey skull compression experiments [16]

Head kinematics

The experimental head accelerations from the JARI head trauma experiments described above were used to validate the response of the monkey head-neck FE model during three simulated head impacts. For this, a model of the impactor and the rubber block used to deliver the impacts at the trauma experiments was generated following the descriptions in the original publication. The initial velocity was prescribed to the rigid impactor and the attached rubber block. The stiffness of the rubber was implemented by adapting the material properties of the rubber block according to the load-deflection curves reported in [6]. Finally, to control the maximum impact stroke, a contact based braking device where the maximum distance could be varied from 10 to 90 mm was included.

To define the position of the head with respect to the impactor, the angle between the Frankfurt plane of the head and the impactor was set to 84 degrees, which was the average value of the 13 cases in which the value was reported. Similarly, an average distance of 28.5 mm between the initial contact point with the head and the lowest horizontal part of the rubber block on the impactor was used. Figure 6 illustrates the positioning of the head-neck model with respect to the impactor as well as the parameters that were used to define the boundary conditions. In addition, since the model only contains the head and the neck down to the 5th cervical vertebra, to simulate the influence of the body on the motion of the head-neck complex, mass and inertial properties were added to a node located in the center of gravity of the monkey's upper body and rigidly attached to the base of the neck. The location of this center of gravity was taken from literature data on anthropometry of the body of macaques by [22]. The inertial properties were estimated based on data from [23]. In this setup, three impacts were simulated:

1. Severe impact speed of 21.7 m/s, with high rubber block stiffness and impact stroke of 30 mm;
2. Medium impact speed of 15.5 m/s, with intermediate block stiffness and impact stroke of 40 mm; and
3. Mild impact speed of 7.5 m/s, with low block stiffness and impact stroke of 60 mm.

The resulting head accelerations from the three simulated cases were compared to the head resultant accelerations from the sagittal impacts that led to concussion, as shown in Figure 11. The simulated impacts produced a fair match with the experimental head resultant accelerations for the whole range of impacts used in this study.

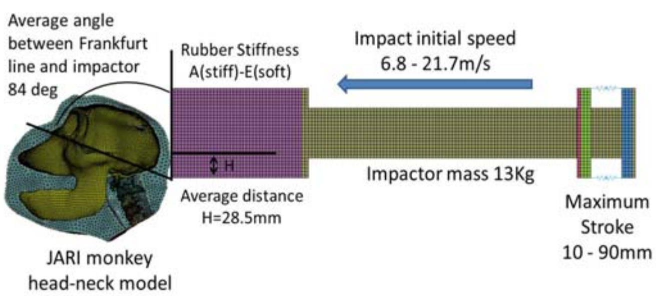

Fig. 10. Scheme of the simulation layout and the parameters used to define the boundary conditions for all the occipital impacts simulated

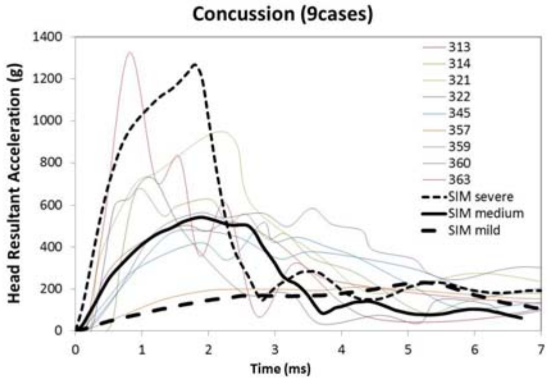

Fig. 11. Experimental acceleration for 9 cases showing concussion and simulation for severe, medium, and mild impacts

Simulation of 19 selected occipital head impacts

Each of the 19 experimental cases was simulated with the validated head-neck model and under the setup previously explained. The angle and distance that define the position of the head-neck model with respect to the impactor were kept constant at 84 degrees and 28.4 mm. The velocity of the impactor just before the impact, the stiffness of the rubber block, and the maximum stroke of the impactor were set case-by-case according to the recorded data presented in Table I. All the 19 simulations were run for the entire time period of contact between the head and the impactor and for at least 2 ms more.

Statistical analysis

The maximum values for the von Mises stress, the principal strain and the strain rate were post processed for each of the brain regions separately. A T-test for significance was carried out to evaluate the difference in the average values between the group with and without concussion. Finally, based on the parameters and regions that showed significant differences, a logistic regression analysis to create the risk curves for concussion was carried out with an open source statistical software package [24].

III. RESULTS

The results from the simulations of the 19 cases are presented in this section. For each brain region, the elements subjected to highest values were identified and the values extracted. Figure 12 shows a representation of the mean values and standard deviations of the maximum values for von Mises stress, principal strain and strain rate in different brain regions. These values are represented separately between the group without concussion (black) and the group with concussion (white).

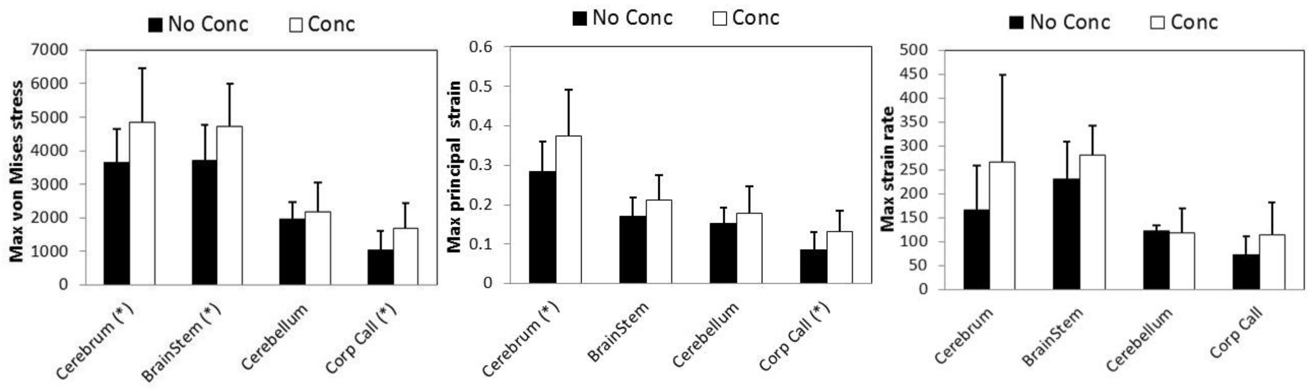

Fig. 12. Mean values and standard deviations for the maximum von Mises stress, principal strain and strain rate grouped according to injury score for all the different brain regions under study. '(*)' indicates the regions for which measured values showed significant difference (P<0.05) for cases with and without concussion.

The results indicate that, at a 95% confidence level, the observed mean values obtained for the two groups were significantly different for the stress in the cerebrum (P=0.030), the brainstem (P=0.031) and the corpus callosum (P=0.038), as well as for the principal strain in the cerebrum (P=0.036) and the corpus callosum (P=0.028). Principal strain in the brainstem (P=0.055) almost reached significance. For the parameters and regions that presented significant differences between concussion and no concussion, the logistic regression analysis was carried out and the probability curve of occurrence of concussion was estimated. Figure 13 shows the obtained probability curves and 95% confidence intervals for the maximum stress and maximum principal strain in the cerebrum, the brainstem, and the corpus callosum.

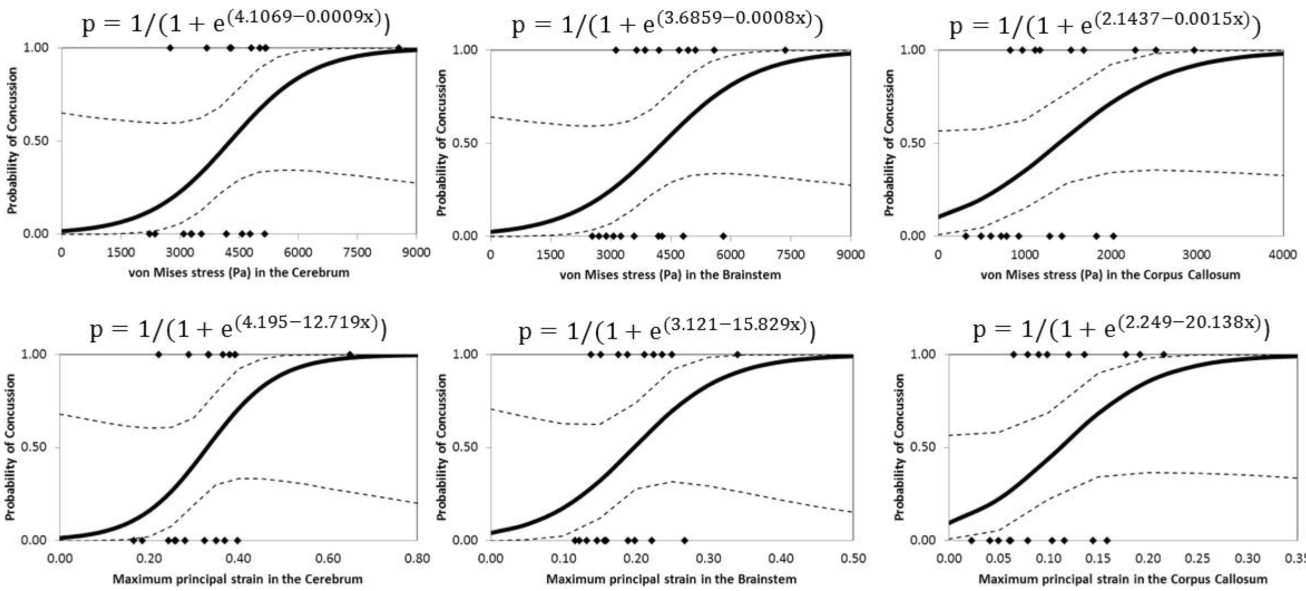

Fig. 13. Probability of concussion (solid line) and 95% confidence intervals (dotted lines) for stress and strain at each of the brain regions

IV. Discussion

Before generating the skull of the FE model, a geometrical analysis of the monkey skull was carried out, based on the CT images. This was done in order to understand the main differences between humans and macaques and to evaluate the availability of experimental data in literature suitable for the validation of the model. From this preliminary study, it was confirmed that the structural constitution of the skull bones differs significantly between humans and macaques. There is consensus within the primatologist community and was mentioned by [2][11] to be an important factor that may affect the difference in response to impacts between small primates and humans. However, the most widely used scaling approaches [9][10] do not consider this issue when scaling brain injury thresholds from primates to humans. It was also confirmed that the skull of the

JARI monkey FE model was very similar in geometry to one of only two skulls from skull compression tests by [16]. Further information showing different skull bone structure between species and a geometrical comparison between the monkey skull model and the skull used for the quasi-static compression experiments is shown in Appendix A. As previously explained, to validate the skull model, experimental data from a quasi-static compression below the threshold for skull fracture were used. The structural behavior of the skull was in accordance with the experiments where low strain values were measured at the top of the skull while higher strain values were observed at the occipital area. Although further validation may be needed to simulate cases involving TBI and skull fractures, since all simulated cases were below the threshold for fracture, we consider the level of validation achieved by the skull sufficient for the purpose of this study.

In a statistical analysis [25] carried out in the past of the original JARI head trauma experimental data, it was observed that the head linear and rotational peak accelerations were highly correlated. This means that it is not possible, based on the experimental results, to distinguish if linear or rotational acceleration contributed to the injury outcome. Both in the simulations and the experiments, the motion of the head was primarily linear during the impact while significant rotation appeared a few milliseconds after the impact. Since both the average case and the 19 case-by-case simulations were simulated for a short time (about 2 ms) after finalisation of the contact with the impactor, the results and conclusions addressed in this study are restricted to the primary loading of the brain under mainly linear acceleration of the skull. We believe that further simulation studies with the monkey FE model can be very helpful in order to isolate and better understand the contribution of the rotational and the linear accelerations of the head on the injury outcome and to clarify the brain loading conditions also in the rebound phase.

Concussion is the most common type of traumatic brain injury. Although there is agreement on the symptoms observed in concussed individuals, there is no general agreement on how to quantify these symptoms. This study is based on a specific technique to evaluate concussion based on changes in vital forms caused by a specific method of delivering the impact to the head, with direct occipital padded impacts, and should be so interpreted. A study of a sub-group of the original trauma experiments similar to the one used for this simulation based study was performed by some of the physicians involved in the trauma experiments in the past [12]. The work focused on an analysis of the concussion output measured by physiological changes and its possible relation to the pathological observations. Based on pathological findings such as hemorrhages or circulatory disturbances seen in the midbrain, pons and medulla oblongata, it was suggested that changes responsible for concussions may have occurred in the brain stem and the cervical cord. The results from the simulation work are consistent with this hypothesis. Both the maximum von Mises stress and maximum principal strain at the brainstem showed significant differences for the groups with and without concussion. The results from the logistic regression analysis suggest a probability of 50% for concussion associated with a stress of 4.2 kPa and a principal strain of 21%. These results seem to be in reasonable accordance with the one only study found in literature in which a NHP FE model was used [26]. In that study, the model was a simplified baboon brain rigidly attached to the skull. It was used to simulate three monkey trauma experimental impacts from [3] with no injury, moderate Diffuse Axonal Injury (DAI) and critical DAI, respectively. Due to the differences in the experimental methods and the injury types observed, a direct comparison with this study is difficult. Still, the suggested levels of 17% strain for the case of no injury, and 28% for the case of moderate injury, seem to agree with the 21% strain level associated with a 50% probability of concussion derived from our study. Also, these findings are consistent with comparable simulation work in the literature in which sports accidents resulting in concussion were reconstructed with human FE models [27][28]. Kleiven [27], based on the simulation of 58 head impacts in American football accidents, identified among others stress at the brainstem as one of the significant predictors for concussion. One more relevant study by Zhang [28], which followed the same methodology as Kleiven, pointed to shear stress in the brainstem as a significant injury predictor.

Although this study presents several limitations, the monkey FE model presented is a unique research tool. According to primatologists, to the effects of brain injury research, Rhesus monkey (Macaca Mulatta) and Japanese monkey (Macaca Fuscata) can be considered within the same macaque species. The fact that these two species were the most widely used for biomechanical studies of brain injuries opens the possibility to perform further research involving not only JARI head trauma experimental data, but some of the other historical experimental series. Summing up all the historical experiments on macaques reported in literature, an estimation of more than 200 specimens and several hundreds of impacts under many different loading conditions leading to different types of injuries may be available [3]-[6]. A joint effort between institutions could throw further valuable light on the TBI research without the need to perform new experiments.

The model and the results presented constitute the first step towards the development of a tissue level injury criterion to extrapolate experimental injury thresholds from animals to humans.

V. LIMITATIONS OF THE STUDY

The fact that several impacts were delivered to the same specimen was shown to be an influencing factor on the injury outcome [25]. This was consistent with some studies in which repeated concussions in the long term (dementia pugilistica) [29] and in the mid and short term (second impact syndrome) [30] showed the importance of considering the possibility of accumulated brain damage. The 19 cases simulated and analysed in this work were based on 7 different specimens. The possible influence of the repeated impacts on the same specimen was not considered in this study, which may be affecting the results. To account for this issue, additional simulations are required to compare response of the cases with a first impact to the cases with subsequent impacts.

The experimental data sources used to define the material properties of the soft tissues of the monkey FE model presented several limitations that may affect the results of this study. On one hand, no detailed information of the variability of geometry, age or gender of the scalp samples used in the tissue compression experiments was available. On the other hand, the brain tissue compression test data used presented substantial variability and only average values were considered in this work. In addition to the sample variability, the relaxation time to 66% indicated in the tests (Figure 7) was in the order of 10 s, which is not typical times relevant for impact tests, which are of shorter time duration.

Finally, how brain-skull interaction is simulated will strongly affect the kinematics of the brain and needs to be properly modelled and validated. The simulation technique used for the skull-brain in the monkey model is in accordance with those commonly used by state-of-the-art human models [27][28]. However, it still presents limitations that may affect to the results of this study. To account for this limitation, a parallel study to analyse the brain-skull interaction considering physiological, biological and biomechanical aspects of relevance has been initiated. In addition, many of the historical experimental data sources that have potential to enhance the validation of the monkey brain-skull interaction, such as the lexan calvarion experiments [31]-[33], head impacts captured by high speed x-ray [34][35], acceleration induced shear strain induced brain hemisections [36] and impedance tests of monkey head-neck [37], among others are currently under study.

VI. CONCLUSIONS

19 monkey head occipital trauma experiments performed in the past have been simulated with a newly developed and validated monkey head-neck FE model. A significant correlation was found between the simulated resulting peak stress-strain values in the brainstem and the occurrence of concussion in the experiments.

VII. ACKNOWLEDGEMENT

We would like to thank the KUPRI for their kind collaboration to obtain the medical images and their valuable advice on comparative anatomy. We also appreciate the support from Marta Gonzalez-Carcedo with the image processing tasks and Dr. Karin Brolin with the writing, both from Chalmers University of Technology.

VIII. REFERENCES

[1] World Health Organization. Global Plan for the Decade of Action for Road Safety 2011-2020.

[2] McElhaney, J, In Search of Head Injury Criteria. John Paul Stapp Memorial Lecture, *Stapp Car Crash Journal*, 49, 2005.

[3] Gennarelli, T, Thibault, L, Tomei, G, et al, Directional dependence of axonal brain injury due to centroidal and non-centroidal acceleration, *Proceedings of 31st Stapp Car Crash Conference*, SAE 872197, 1987.

[4] Ommaya, A, Hirsch, A, Tolerances for cerebral concussion from head impact and whiplash in primates, *Journal of Biomechanics*, volume 4, issue 1, 1971.

[5] Stalnaker, R, Melvin, J, Nusholtz, G, et al, Head Impact Response, SAE Technical Paper 770921, 1977.

[6] Ono, K., Kikuchi, A, Nakamura, M, et al, Human Head Tolerance to Sagittal Impact: Reliable Estimation deduced from Experimental Head Injury using Subhuman Primates and Human Cadaver Skulls. *Proceedings of 24th Stapp Car Crash Conference*, SAE 801302, 1980.

[7] Kikuchi A, Ono K, Nakamura N, et al, Human head tolerance to lateral impact reduced from experimental head injuries using primates, *Proceedings of the Ninth Technical Conference on Experimental Safety Vehicles*, November 1982.

[8] Sakai, H, Nakamura, N, Sekino, H, et al, Experimental Head Injury with Lateral Impact Using Monkeys – Dynamic and Pathological Investigation, *Neurologia medico-chirurgica*, volume 22, issue 7, 1982.

[9] Holbourn, Mechanics of Head Injuries, pages 438-440, *The Lancet*, October 1943.

[10] Stalnaker, R, McElhaney, J, Roberts, V, MSC Tolerance Curve for Human Head Impacts, ASME 1971.

[11] Ommaya, A, Hirsch, A, Protection of the brain from Injury during Impact: Experimental Studies in the Biomechanics of Head Injury, *AGARD Conference*, 1971.

[12] Kanda, R, Nakamura, N, Sekino, H, et al, Experimental head injury in monkeys - concussion and its tolerance level. *Neurologia medico-chirurgica*, volume 21, 1981.

[13] Committee on Terminology in Neurotraumatology (Glossary) of the World Federation of Neurological Society: Glossary of Neurotraumatology. *Acta Neurochirurgica [Suppl]*, volume 25, 1979.

[14] BrainInfo (1991- present), National Primate Research Center, University of Washington, Internet: [http://www.braininfo.org], Date Updated [31st of May, 2012].

[15] Digital Morphology Museum, Primate Research Institute, Kyoto University, Internet: [http://www.pri.kyoto-u.ac.jp/dmm/WebGallery/index.html], Date Updated [31st of May, 2012].

[16] Stalnaker, R, et al, Validation Studies for Head Impact Injury Model, Contract No.DOT-HS-031-3-749, Final Report, September 1977.

[17] Mao, H, Zhang, L, Yang, K, et al, "Application of a Finite Element Model of the Brain to Study Traumatic Brain Injury Mechanisms in the Rat", *Stapp Car Crash Journal*, volume 50, 2006.

[18] McElhaney, J, Roberts, V, Hilyard, F, Handbook of Human Tolerance, pages 124-174, *JARI*, Japan, 1976.

[19] Galford, J, McElhaney, J, A viscoelastic study of scalp, brain, and dura. *Journal of Biomechanics*, volume 3, issue 2, 1970.

[20] Melvin, J, McElhaney, J, and Roberts, V, Development of a Mechanical Model of the Human Head - Determination of Tissue Properties and Synthetic Substitute Materials, SAE 700903, 1970.

[21] Arbogast, K, Margulies, S, Material characterization of the brainstem from oscillatory shear tests, *Journal of Biomechanics*, volume 31, issue 9, 1998.

[22] Vilensky, J, Masses, centers-of-gravity, and moments-of-inertia of the body segments of the rhesus monkey (Macaca mulatta). *American Journal of Physical Anthropology*, volume 50, pages 57–65, 1979.

[23] Ogihara, N, Makishima, H, Aoi, S, et al, Development of an anatomically based whole-body musculoskeletal model of the Japanese macaque (Macaca fuscata). *American Journal of Physical Anthropology*, volume 139, 2009.

[24] R Development Core Team, R: A language and environment for statistical computing. R Foundation for Statistical Computing, Internet: [http://www.R-project.org], Date Updated [31st of May, 2012].

[25] Vander Vorst, M, Ono, K, Chan, P, and Stuhmiller, J, Correlates to traumatic brain injury in nonhuman primates, *The Journal of Trauma-Injury, Infection, and Critical Care*, volume 62, 2007.

[26] Mendis, Finite Element Model of the Brain to establish Diffuse Axonal Injury Criteria. Ohio State University PhD dissertation, 1992.

[27] Kleiven, S, Predictors for traumatic brain injuries evaluated through accident reconstructions. *Stapp Car Crash Journal*, 51, 2007.

[28] Zhang, L, Yang, K, King, A, A Proposed Injury Threshold for Mild Traumatic Brain Injury. *Journal of Biomechanical Engineering*, volume 126, issue 2, 2004.

[29] Erlanger, D, Kutner, K, Barth, J, et al, Neuropsychology of sports-related head injury: dementia pugilistica to postconcussion syndrome, *The Clinical Neuropsychologist*, volume 13,1999.

[30] Cantu, R, Second-Impact syndrome, *Clinics in Sports Medicine*, volume 17, issue 1, 1998.

[31] Pudenz, RH, Sheldon, CH, The Lucite calvarion; a method for direct observation of the brain; cranial trauma and brain movement. *Journal of Neurosurgery*, volume 3, issue 6, Nov 1946.

[32] Ommaya, A, Boretos, J, Beile E, The Lexan calvarium: an improved method for direct observation of the brain. *Journal of Neurosurgery*, volume 30, issue 1, 1969.

[33] Gosch, H, Gooding, E, Schneider, R, The Lexan Calvarium for the Study of Cerebral Responses to Acute Trauma, *Journal of Trauma-Injury, Infection and Critical Care*, volume 10, issue 5, 1970.

[34] Nusholtz, G, Melvin, J, Alem, N, Head Impact Response Comparisons of Human Surrogates, SAE 791020, 1979.

[35]Ommaya, A, Experimental head injury in the monkey, Head Injury, pages 260-275, *W.F.Caveness and A.E Walker*, Philadelphia, 1966.
[36]Hodgson, V, Thomas, L, Acceleration Induced Shear Strains in a Monkey Brain Hemisection, SAE 791023, 1979.
[37]Stalnaker, R, McElhaney, J, Head Injury Tolerance for Linear Impacts by Mechanical Impedance Methods, ASME 1970.

IX. APPENDIX A. SKULL BONE STRUCTURE AND SKULL DIMENSIONS

Figure 14 shows a comparison of the profile of grey densities typically observed in the frontal bone of the skull of humans in comparison to macaques. It can be observed that for humans the grey density drops in the area corresponding with the trabecular bone. However, this drop is not observed in the monkey CT image.

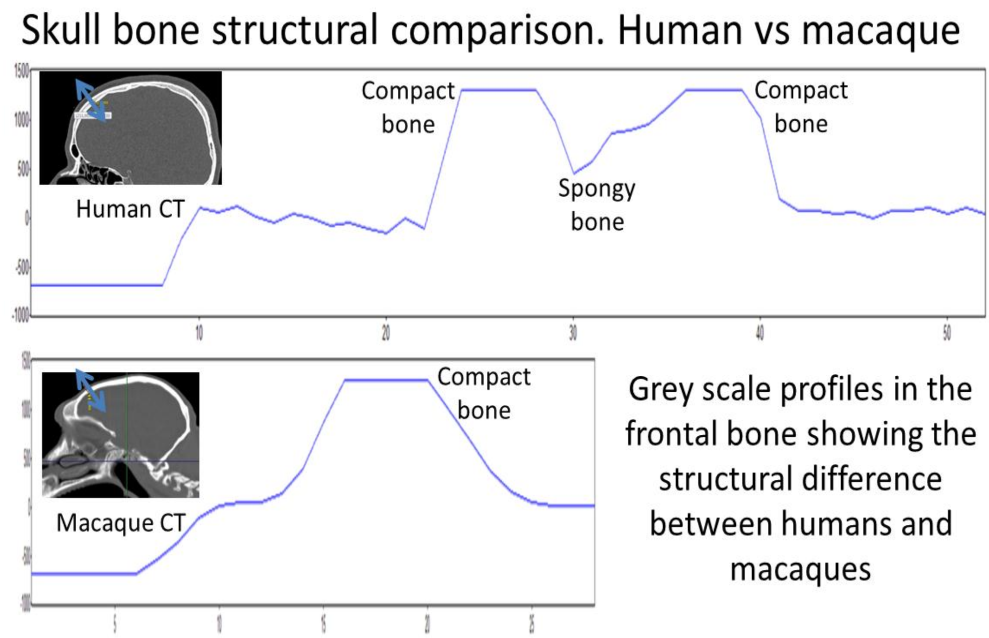

Fig 14. Human vs. macaque skull bone structural

Figure 15 shows a comparison between the skull dimensions as reported by Stalnaker [16] at quasi-static compression tests in comparison with the skull FE model developed. External length and width dimensions are close to each other and the skull variable thickness profiles follow similar patterns.

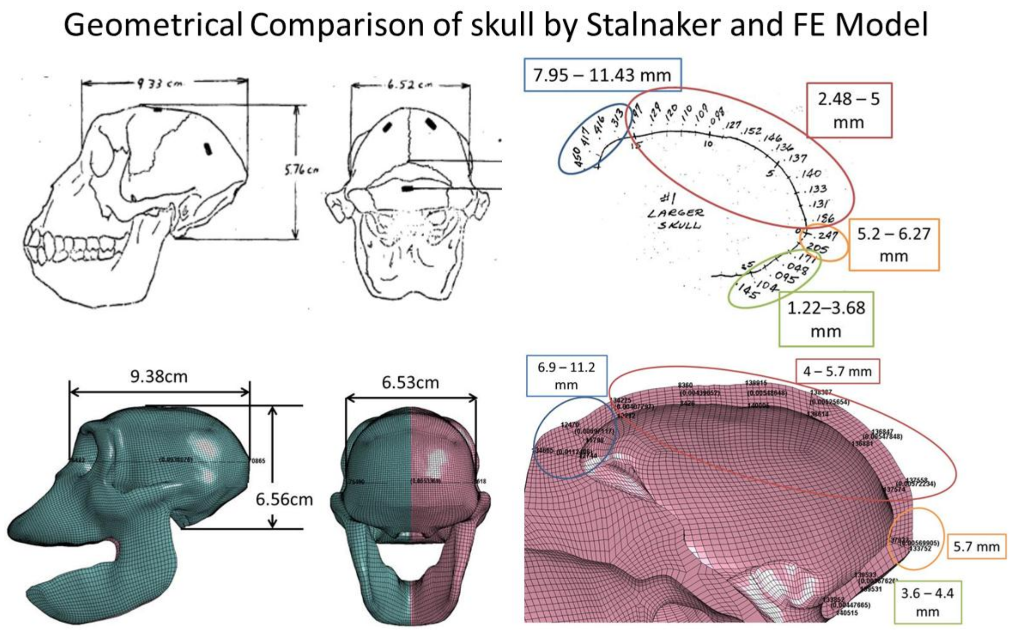

Fig. 15. Geometrical comparison between the skull used by Stalnaker [16] in the quasi/static compression tests and the skull FE model.